An Algorithm for Discrete Constant Mean Curvature Surfaces

Bernd Oberknapp* Konrad Polthier†

April 25, 1997‡

Abstract. We present a new algorithm for computing discrete constant mean curvature surfaces in $\mathbb{R}^3$. It is based on the definition of a discrete version of the conjugate surface construction for CMC surfaces. Here we solve a Plateau problem for a discrete minimal surface in $\mathbb{S}^3$ by computing a sequence of discrete harmonic maps $F_i : \mathbb{S}^3 \to \mathbb{S}^3$. The definition of a discrete conjugation allows to transform this sequence to a sequence of conjugate discrete maps which converges to a discrete CMC surface in $\mathbb{R}^3$. The algorithm is applicable to free boundary value problems for CMC surfaces and led to the recent discovery of new compact CMC surfaces.

1. Introduction

Surfaces with constant mean curvature (CMC surfaces) are the mathematical abstraction of physical soap films and soap bubbles. Such surfaces behave like rubber bands which try to contract under their surface tension and thereby to minimize their total surface area under the restriction of enclosing a given amount of volume. The restriction can also be interpreted as a constant difference in pressure on the two sides of the surface – for minimal surfaces the difference is zero. The simplest CMC surface is the sphere, the typical example of a soap bubble. More complicated examples, especially compact ones (i.e. finite and without boundary), are already hard to find and must have self-intersections.

The global condition of "area minimizing under volume constraint" implies a necessary local condition that must be fulfilled at every point: the mean curvature $H = \frac{1}{2}(\kappa_1 + \kappa_2)$, the mean of the two principal curvatures, must be constant on the surface. The differential geometric description of CMC surfaces originates from this local property and therefore defines a class of surfaces which covers more than the set of physically existing soap bubbles. In general, the characterisation of "area minimizing under volume constraint" is no longer true from a global point of view, since differential geometric CMC surfaces may have self-intersections and extend to infinity. But locally every small neighbourhood of a point is still area minimizing while fixing the volume which is enclosed by the cone defined by the neighbourhood's boundary and an arbitrary point in $\mathbb{R}^3$.

There have been a number of approaches to compute CMC surface numerically. For example the evolver of Brakke [3] is an efficient tool, see e.g. its application to

*Supported by SFB 256 at Universität Bonn

†Partially supported by SFB 288 at Technische Universität Berlin

‡To appear in: Visualization and Mathematics, Eds: H.C. Hege and K. Polthier, Springer 1997

foam problems in [4]. Other methods apply finite element techniques to the partial differential equation of CMC surfaces. Heil [10] computes CMC tori by making use of an explicit representation in terms of theta functions. In general, direct approaches of minimizing surface area under volume constraint are faced with stability problems. More complicated free boundary value problems are usually instable w.r.t. the variational problem, they degenerate or converge to a solution of a simpler boundary value problem. Different discrete approaches are Bobenko and Pinkall [2] for isothermic surfaces and Hoffmann [11] who discretizes the Dorfmeister-Pedit-Wu recipe of CMC surfaces – both methods rely on quadrilateral meshes.

Our approach differs mainly in two aspects from previous algorithms. The first difference is that we do not solve the problem for a CMC surface in $\mathbb{R}^3$ directly, but we start with a corresponding problem for a minimal surface in $\mathbb{S}^3$, the unit sphere in $\mathbb{R}^4$. It is known from differential geometry that there is a 1–1 correspondence between Euclidean CMC surfaces and minimal surfaces in $\mathbb{S}^3$. On the one hand this method converts an instable problem with Neumann boundary conditions in $\mathbb{R}^3$ into a problem with Dirichlet boundary conditions in $\mathbb{S}^3$ which often is stable. But on the other hand one is faced with the new problem of describing the transformation from a spherical minimal surface to a Euclidean CMC surface, the so-called *conjugation*. The conjugate surface construction has been described and applied in several works and led to the discovery and existence proof of minimal and CMC surfaces in $\mathbb{R}^3$ [12], $\mathbb{S}^3$ [13] [6] [7] and $\mathbb{H}^3$ [15]. It is applied to highly symmetric surfaces where the symmetry lines divide the wanted surface in fundamental patches, thereby reducing the problem to the construction of such a fundamental patch. Our algorithm is designed to cover such problems for CMC surfaces.

The second difference of our approach is the application of *discrete techniques*. Here *discrete* is used in a different sense than in finite element theory: we additionally redefine geometric properties in terms of the discrete surface which allows to operate *exactly* on these data. The conjugate surface construction resisted numerical approaches for a long time because the conjugation was originally defined using second derivatives of the spherical minimal surface which itself is the (inaccurate) result of a numerical algorithm – the accumulative loss of accuracy prohibited an application of standard techniques. But even with the C^1 description of the conjugation (lemma 1) the application of discrete techniques is the essential point. We extend the concept of discrete surfaces which was introduced for harmonic maps and minimal surfaces in Pinkall and Polthier [14] to both problems, solving the Plateau problem in $\mathbb{S}^3$ and computing the conjugate surface. Especially for the conjugation process our discrete concept provides *exact* results for important geometric properties.

It should be noted that with the algorithm a large number of known CMC surfaces can be computed for the first time. The algorithm was also used in the recent discovery of compact CMC surfaces with low genus [7] [9].

The algorithms were implemented in the mathematical visualization environment GRAPE [17] developed at the Sonderforschungsbereich 256 at the University of Bonn. Besides other tools there are numerical algorithms and visualization methods implemented for the experimental study of differential geometric surfaces [1], e.g. parameter-dependent surfaces, curvature dependent adaptive refinement and surface builder for creating initial triangulations. The first author has implemented the extensions for surfaces in $\mathbb{S}^3$ and the numerics for computing discrete minimal surfaces in $\mathbb{S}^3$ and their conjugate CMC surfaces in $\mathbb{R}^3$.

2. PREREQUISITES

We start with some necessary differential geometric prerequisites for our algorithm which are well-known in the smooth case except for the C^1 description of the conjugation (lemma 1). First we recall the 1–1 correspondence between CMC surfaces in $\mathbb{R}^3$ and minimal surfaces in $\mathbb{S}^3$, and second we discuss consequences of the Lie group structure of $\mathbb{S}^3$.

Let $F : \Omega \to M$ be a minimal surface in $\mathbb{S}^3$ parametrized over a domain $\Omega \subset \mathbb{R}^2$. M is characterized by its metric tensor $g = \langle \partial F, \partial F \rangle$ and its second fundamental form $b = \langle \partial^2 F, N \rangle$, where $N(p) \in T_{F(p)}\mathbb{S}^3$ is the normal vector of M at a point $F(p)$. Let $S = bg^{-1}$ be the Weingarten operator, then the mean curvature is $H = \frac{1}{2}\,\mathrm{trace}\, S$. The CMC surface $M^* \subset \mathbb{R}^3$ corresponding to M is given by the geometric data

$$\begin{array}{rcl} g^* & = & g \\ S^* & = & JS + \mathrm{id}, \end{array} \tag{1}$$

where J_p is the rotation by $\frac{\pi}{2}$ in the oriented tangent space $T_p\Omega$ and id_p the identity map of $T_p\Omega$ at a point $p \in \Omega$. It can easily be proved that the geometric data (g^*, S^*) integrates over Ω to a CMC surface M^* and that M^* is unique up to Euclidean motions [12]. Conversely, every CMC surface in $\mathbb{R}^3$ has a corresponding minimal immersion in $\mathbb{S}^3$.

Remark 1. *For the conjugate surface construction the correspondence of the boundaries of M and M^* is essential (see section 5). If M is bounded by an embedded spherical polygon of great circle arcs then M^* is bounded by geodesic curvature lines (planar symmetry lines of the CMC surface) and vice versa [12]. Since M and M^* are isometric, corresponding boundary arcs have the same lengths and the angles at corresponding vertices – the angles of the spherical polygon and the angles between the planar symmetry lines (the dihedral angles of their symmetry planes) – are identical.*

Remark 2. *The CMC surface $M^* \subset \mathbb{R}^3$ generated by conjugation of a minimal surface $M \subset \mathbb{S}^3$ is NOT the stereographic projection of M into $\mathbb{R}^3$ (stereographic projection is not an isometry). Nevertheless stereographic projection of minimal surfaces in $\mathbb{S}^3$ into $\mathbb{R}^3$ leads to interesting surfaces which are critical points of the Willmore energy in $\mathbb{R}^3$ but this is different from our theme.*

The description (1) of the conjugation uses C^2 information of the surface M. For this reason the conjugation resisted numerical approaches for a long time.

We proceed with a more suitable C^1 description of the conjugation process and recall the group representation of $\mathbb{S}^3$. As a model we identify $\mathbb{S}^3$ with the unitary quaternions

$$\mathbb{S}^3 \approx \left\{ x = x_0 + x_1\mathbf{i} + x_2\mathbf{j} + x_3\mathbf{k} \;\middle|\; \sum_{i=0}^{4} x_i^2 = 1 \right\}$$

where $\{\mathbf{i}, \mathbf{j}, \mathbf{k}\}$ are the imaginary units. The quaternionic left multiplication induces a Lie group structure on $\mathbb{S}^3$: every point $p \in \mathbb{S}^3$ defines a map

$$\begin{aligned} p : \mathbb{S}^3 &\rightarrow \mathbb{S}^3 \\ q &\mapsto pq \end{aligned}$$

by left multiplication. Its differential map dp also operates by quaternionic left multiplication

$$\begin{aligned} dp : T_q\mathbb{S}^3 &\rightarrow T_{pq}\mathbb{S}^3 \\ v &\mapsto pv. \end{aligned}$$

The geometric effect of the differential map dp on tangent vectors is as follows: let $v \in T_q\mathbb{S}^3$ and γ be the geodesic segment from q to pq with length l. Then pv is obtained by parallel translation of v along γ and left rotation around γ' about an angle l. We call this operation *left translation* of the vector v along γ. The point $id := (1, 0, 0, 0) \in \mathbb{S}^3$ serves as the identity element and will henceforth be called *identity* of $\mathbb{S}^3$.

The Lie algebra of $\mathbb{S}^3$ is identified with the tangent space $T_{id}\mathbb{S}^3$. For every vector $v \in T_p\mathbb{S}^3$ there exists a representative $\mathfrak{v} \in T_{id}\mathbb{S}^3$ in the Lie algebra given by

$$\mathfrak{v} = p^{-1}v$$

where p^{-1} is the inverse element of p.

With this notation at hand we can formulate the following C^1 correspondence which does not seem to have appeared in the literature, see the remark below.

Lemma 1. *Let $\Omega \subset \mathbb{C}$ be a simply connected domain and $F : \Omega \rightarrow \mathbb{S}^3$ a minimal immersion. We identify $\mathbb{S}^3$ with the unitary quaternions. Then the conjugate* CMC *surface $F^* : \Omega \rightarrow \mathbb{R}^3$ with $H = 1$ is (up to congruence of $\mathbb{R}^3$) given by*

$$F^*(z) := \operatorname{Im} \int_\gamma F^{-1} {*dF} \tag{2}$$

where γ is an arbitrary path in Ω from a fixed point z_0 to z. The map Im *denotes the standard identification of $T_{id}\mathbb{S}^3$ with $\mathbb{R}^3$, resp. the imaginary part of quaternions. $*$ is the Hodge star operator in Ω.*

Proof. Equation (2) is the integral representation of the following differential system

$$\begin{aligned} dF^* &= \operatorname{Im} F^{-1} {*dF} \\ N^* &= \operatorname{Im} F^{-1} N, \end{aligned}$$

where $N \in T\mathbb{S}^3$ is the normal field of F. Since F is minimal in $\mathbb{S}^3$ we have $\Delta_g F = -2F$ and easily obtain that the system is integrable to a smooth surface in $\mathbb{R}^3$.

To prove that F^* is CMC we make use of the identity $\Delta_g F^* = 2HN^*$ for the Laplace-Beltrami operator of any smooth surface in $\mathbb{R}^3$ and show that $H = 1$ holds. Let F be a conformal immersion with induced metric $g = E\ dw^2$ in Ω with local coordinates $w = (u, v)$. Then $*$ acts by rotation by -90 degrees in the oriented tangent space of $F(\Omega)$ and by using the identities $*F_u = -F_v$, $*F_v = F_u$, $(F^{-1})_u = -F^{-1}F_uF^{-1}$, $F^{-1}F_uF^{-1}F_u = -E\ id$ and $F^{-1}F_uF^{-1}F_v = EF^{-1}N$ we obtain:

$$\begin{aligned} \Delta_g F^* &= \frac{1}{E}(F^*_{uu} + F^*_{vv}) = \operatorname{Im} \frac{1}{E}((F^{-1}{*F_u})_u + (F^{-1}{*F_v})_v)) \\ &= \operatorname{Im} \frac{1}{E}(-(F^{-1}F_v)_u + (F^{-1}F_u)_v)) \\ &= \operatorname{Im} \frac{1}{E}(F^{-1}F_uF^{-1}F_v - F^{-1}F_{vu} - F^{-1}F_vF^{-1}F_u + F^{-1}F_{uv}) \\ &= \operatorname{Im} \frac{2}{E}F^{-1}F_uF^{-1}F_v = \operatorname{Im} 2F^{-1}N \\ &= 2N^*. \end{aligned}$$

Therefore F^* is a CMC surface with $H = 1$.□

Remark 3. *Originally, Lawson [13] described the conjugation process via equations (1). Karcher [12] found a C^1 construction using Hopf vector fields to describe the spherical boundary of the accompanying minimal surface in $\mathbb{S}^3$ in terms of the Euclidean boundary of the wanted CMC surface – this established the conjugate surface construction as a powerful constructive method (cf. section 5). Pinkall saw that the C^1 formulation also holds in the interior of the surface. Bobenko uses a different C^1 description.*

In the following we do not distinguish an orientation of the surfaces, therefore the computations are valid up to sign.

Our discrete description of formula (2) turns out to be ideal for a numerical algorithm (cf. section 4).

3. Discrete Harmonic Maps and Minimal Surfaces in $\mathbb{S}^3$

In this section we define discrete surfaces as it is done in finite element theory. The difference to the finite element approach is that we additionally redefine geometric properties in terms of the discrete surface instead of trying to approximate the definitions from the continuous case within a finite dimensional function space. In that case the geometric terms would not be available on the discrete level while our approach allows to operate entirely on the discrete level and therefore to be *exact* on the discrete data. The most remarkable use of this approach in our paper is the definition of the conjugation process from a minimal surface to a constant mean curvature surface (cf. section 4).

We start by defining the class of surfaces and discrete maps we will consider. We restrict to Euclidean space $\mathbb{R}^3$ and to the unit sphere $\mathbb{S}^3 \subset \mathbb{R}^4$, but many definitions generalize to other ambient spaces.

Definition 2. *A* discrete surface, or triangulation, in $\mathbb{R}^3$ or $\mathbb{R}^4$ *is a topological simplicial complex consisting of triangles where every edge belongs to at most two triangles. Triangles may degenerate to line segments or points. A* discrete surface in $\mathbb{S}^3$ *is a discrete surface in $\mathbb{R}^4$ with all vertices lying on the unit sphere of $\mathbb{R}^4$ (i.e. we do not use geodesic triangles in $\mathbb{S}^3$).*

Let $\mathfrak{T}(\mathbb{R}^3)$, $\mathfrak{T}(\mathbb{R}^4)$ and $\mathfrak{T}(\mathbb{S}^3)$ denote the corresponding classes of triangulations, and let $\mathfrak{T}$ be a placeholder for any one of these three classes.

Remark 4. *The discussions in this chapter are valid for triangulations where more than two triangles join a common edge, see [14] for examples. But since we cannot extent conjugation to these surfaces we exclude them already at this point.*

Remark 5. *In section 4 we extent the definition of a discrete surface to non-triangulated surfaces, namely the edge graph of the conjugate* CMC *surface of a minimal surface which is dual to the edge graph of the minimal surface.*

Definition 3. *Let $N, M \in \mathfrak{T}$ be two triangulations having the same underlying topological structure, then the pair of surfaces defines a natural* discrete map $F : N \to M$*: if $\{\triangle_i^N\}$ resp. $\{\triangle_i^M\}$ are the set of triangles of N resp. M, then F is defined by* atomic maps $f_i : \triangle_i^N \to \triangle_i^M$ *which map every vertex of $\triangle_i^N$ to its corresponding vertex in $\triangle_i^M$ and extend as linear maps into the interior of $\triangle_i^N$.*

Discrete harmonic maps play an essential part in our algorithm: we obtain minimal surfaces as limit sets of sequences of harmonic maps and also define the discrete conjugation algorithm for harmonic maps. Smooth harmonic maps are characterized by several equivalent criteria, e.g. as solutions of the Laplace equation, as critical points of the Dirichlet energy or by the mean value property. The variational formulation using the Dirichlet energy can be extended to an explicit criterion for discrete surfaces, namely a balancing condition involving weighted edge lengths (compare corollary 9 for the discrete mean value property).

Definition 4. *The* Dirichlet energy *of a discrete map $F : N \to M$, $N, M \in \mathfrak{T}$, is defined as the sum of the well-defined Dirichlet energies of its differentiable atomic maps*

$$E_D(F) = \frac{1}{2}\int_N |\nabla F|^2 := \frac{1}{2}\sum_i \int_{\triangle_i^N} |\nabla f_i|^2 .$$

The Dirichlet energy of a map into $\mathfrak{T}(\mathbb{S}^3)$ is defined as its energy as a map into $\mathfrak{T}(\mathbb{R}^4)$.

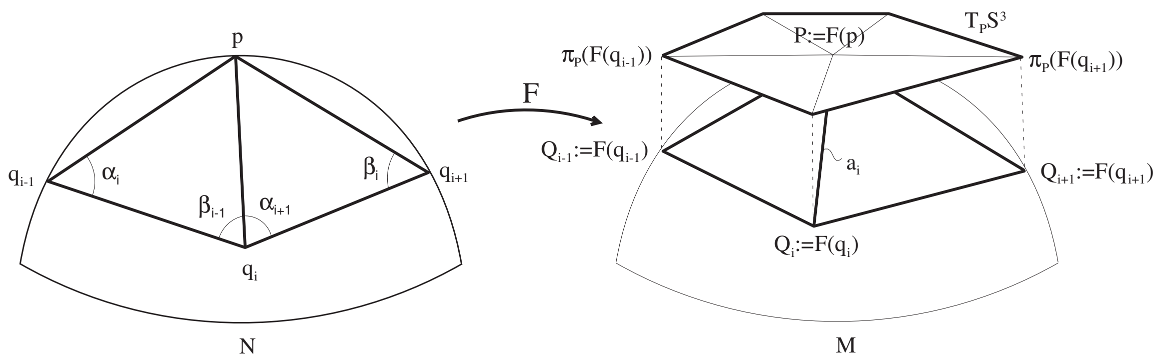

Figure 1: Notation for the discrete map $F : N \to M$.

Remark 6. *Like for smooth surfaces the Dirichlet energy of the identity map* id : $M \to M$ *of a discrete surface* $M \in \mathfrak{T}(\mathbb{S}^3)$ *is identical to the area of* M *defined as*

$$\operatorname{area}(M) = \sum_{\Delta_i^M \subset M} \operatorname{area}(\Delta_i^M), \tag{3}$$

where the area of the atomic triangles Δ_i^M *is measured in* $\mathbb{R}^4$.

From the paper of Pinkall and Polthier [14] we recall the following theorem which allows us to represent the Dirichlet energy of a discrete map between two triangulations using geometric terms of the discrete data.

Theorem 5. *The Dirichlet energy of a discrete map* $F : N \to M$, $N, M \in \mathfrak{T}$, *is given by*

$$E_D(F) = \frac{1}{2}\int_N |\nabla F|^2 = \frac{1}{4}\sum_{\text{edges } a_i} (\cot\alpha_i + \cot\beta_i)\,|a_i|^2\,, \tag{4}$$

where a_i *runs through all edges of* M *and* α_i, β_i *denote the two angles in* N *opposite to* $F^{-1}(a_i)$ *measured in* $\mathbb{R}^4$, *see figure 1 for the notation. For edges at the boundary of* M *one of the two* cot *values is missing.*

From now on we restrict ourself to discrete maps $F : \mathfrak{T}(\mathbb{S}^3) \to \mathfrak{T}(\mathbb{S}^3)$ to avoid case distinctions. For the Euclidean case $\mathfrak{T}(\mathbb{R}^3)$ we refer to [14].

Definition 6. *A discrete map* $F : N \to M$ *is* discrete harmonic *if it is a critical point of the Dirichlet energy functional* E_D *with respect to variations of image points in* M. *For* $M \in \mathfrak{T}(\mathbb{S}^3)$ *we restrict the variational directions to be tangential to* $\mathbb{S}^3$.

Further we restrict variational directions of boundary points to respect symmetry properties. This allows to extend harmonic maps as harmonic maps across symmetry arcs of the boundary:

(1) *If the boundary is a* straight line *in* $\mathbb{S}^3$ *its vertices are allowed to move on the geodesic of* $\mathbb{S}^3$*, i.e. on a great circle. This is the only case relevant for the conjugate surface construction, it ensures that the* CMC *surfaces in* $\mathbb{R}^3$ *will be bounded by planar symmetry arcs.*

(2) *If the boundary is* planar symmetric *its vertices are allowed to move on a totally geodesic hyperplane of* $\mathbb{S}^3$*, i.e. on a suitable* $\mathbb{S}^2$*.*

(3) *For all other boundaries the vertices are not allowed to move.*

By differentiating equation (4) with respect to vertices in image space we obtain a local formula for the critical points of the Dirichlet functional. We restrict ourself to interior vertices of the triangulation to avoid the obvious case distinctions at boundary vertices.

For $p, q \in \mathbb{S}^3$ the map

$$\begin{aligned} \pi_p : \mathbb{S}^3 &\rightarrow T_p\mathbb{S}^3 \\ q &\mapsto q - \langle q, p \rangle\, p \end{aligned} \tag{5}$$

projects the point q to its part orthogonal to the point p. It can also be interpreted as the projection

$$\begin{aligned} \pi_p : T_p\mathbb{R}^4 &\rightarrow T_p\mathbb{S}^3 \\ q - p &\mapsto \pi_p(q). \end{aligned} \tag{6}$$

of the vector $q - p \in T_p\mathbb{R}^4$ emanating from p onto its tangential component in $T_p\mathbb{S}^3$.

Theorem 7 [Balancing Condition]**.** *Let* $F : N \rightarrow M$*,* $N, M \in \mathfrak{T}(\mathbb{S}^3)$*, be a discrete map in* $\mathbb{S}^3$*. Then* F *is harmonic iff at every interior point* $P \in M$

$$\frac{1}{2} \sum_{\substack{\text{neighbour} \\ \text{vertices } Q_i \text{ of } P}} (\cot \alpha_i + \cot \beta_i)\; \pi_P(Q_i - P) = 0 \tag{7}$$

holds. As above the angles α_i *and* β_i *are measured in the domain* N *as angles in* $\mathbb{R}^4$*, see figure 1 for the notation.*

Proof. The equation follows directly by differentiating equation (4) and taking the tangential part w.r.t. $\mathbb{S}^3$ as defined by (5).□

Remark 7. *If one extends a surface with a symmetry arc as boundary curve by reflection then the boundary vertices become interior points of the extended surface. The important result is that equation (7) holds at these points, too. This is an immediate result from the boundary conditions in definition 6 and justifies the restrictions we imposed there.*

We now state two lemmas showing that our definition of discrete harmonicity preserves similar properties of the continuous case.

Corollary 8. *Let $F : N \to M$, $N, M \in \mathfrak{T}(\mathbb{S}^3)$, be a discrete harmonic map in $\mathbb{S}^3$ and let $\{Q_i\}$ be the set of neighbour points of an interior vertex P in the image of F. If all points Q_i and P lie in a hemisphere of $\mathbb{S}^3$ and all angles $\{\alpha_i, \beta_i\}$ in the parameter domain N are acute, then P lies in the convex hull of the points $\{Q_i\}$ in $\mathbb{S}^3$.*

Proof. Inserting definition (5) of the projection operator π_P we can rearrange the minimality condition (7) to

$$P = \sum_i \frac{\cot \alpha_i + \cot \beta_i}{\sum_j \cot \alpha_j + \cot \beta_j} Q_i + \lambda P \tag{8}$$

where

$$\lambda = \frac{\sum_i (\cot \alpha_i + \cot \beta_i) \langle Q_i - P, P \rangle}{\sum_i \cot \alpha_i + \cot \beta_i}.$$

Since all angles are assumed to be acute all coefficients are in $[0, 1]$ and equation (8) is a convex combination of the points Q_i plus an additional term λP parallel to P. Therefore P lies in the Euclidean cone spanned by the vertices $\{Q_i\}$ and therefore also in their spherical convex hull.□

The mean value property of smooth harmonic maps is well-known. The following lemma states an equivalent for discrete harmonic maps.

Corollary 9. *Let the points $\{q_i\}$ form a regular n-sided polygon with center p in N, and let $F : N \to M$, $N, M \in \mathfrak{T}(\mathbb{S}^3)$, be a discrete harmonic map. Then $P := F(p)$ is the mean value of the points $Q_i := F(q_i)$ up to some multiple of P*

$$P = \frac{1}{n} Q_i + \lambda P.$$

with λ as in (8).

Proof. All angles occurring in equation (8) are identical because the domain polygon is regular.□

Using theorem 7 we can define discrete minimal surfaces in $\mathbb{S}^3$ by a variational characterization.

Definition 10 [Discrete Minimal Surface in $\mathbb{S}^3$]**.** *A triangulation $M \in \mathfrak{T}(\mathbb{S}^3)$ is a* discrete minimal surface in $\mathbb{S}^3$ *if it is a critical point of the area functional (3) w.r.t. variation of its vertices in $\mathbb{S}^3$.*

It can easily be shown that this condition is equivalent to equation (7) with both angles and vertices measured in $M \subset \mathbb{R}^4$.

We now proceed to compute minimal surfaces in $\mathbb{S}^3$ by applying an iteration process as introduced in Dziuk [5] for minimal surfaces in Euclidean space, see also Pinkall and Polthier [14].

In the smooth case it is well-known that the image of a conformal harmonic map is a minimal surface and that the Dirichlet energy of a map is equal to the sum of the area of the image and the so-called conformal energy of the map. We iteratively compute harmonic maps which converge to a conformal harmonic map, i.e. to a minimal surface, in the limit.

Problem: Let Γ be a curve in $\mathbb{S}^3$, then we are looking for a discrete minimal surface with boundary Γ (for simplicity we restrict to a Plateau problem with Dirichlet boundary conditions).

Minimal Surface Construction:

(1) Let $M_0 \in \mathfrak{T}(\mathbb{S}^3)$ be an arbitrary initial surface with boundary $\partial M = \Gamma$.

(2) Let M_i be a surface with boundary Γ, then compute the surface M_{i+1} as the minimizer of

$$E_D(F : M_i \to M_{i+1}) = \min_{\substack{M \in \mathfrak{T}(\mathbb{S}^3) \\ \partial M = \Gamma}} E_D(F : M_i \to M).$$

This defines a map $F_i : M_i \to M_{i+1}$.

(3) As long as $|M_{i+1} - M_i| > \varepsilon$ in some suitable norm continue with step (2) and $i \to i + 1$.

This algorithm generates a sequence of discrete surfaces $\{M_i\}$ and harmonic maps $\{F_i\}$ and leads to a discrete minimal surface M:

Theorem 11. *A subsequence of the discrete surfaces $\{M_i\}$ generated by the above algorithm converges to a discrete minimal surface $M \in \mathfrak{T}(\mathbb{S}^3)$ if no triangles degenerate. The corresponding sequence of harmonic maps $\{F_i\}$ converges to the identity map* $\mathrm{id} : M \to M$.

Proof. With minor modifications the corresponding proof in [14] can directly be extended to $\mathbb{S}^3$. The trick of changing the domain from M_i to M_{i+1} after each step has the same effect as making the new initial map conformal by modifying the domain. But the change of the domain in step (2) generates a true conformal initial map, namely the identity map $\mathrm{id} : M_i \to M_i$.□

Remark 8. *Instead of approximating a smooth solution of the Plateau problem as it is done in finite element theory we compute an approximation of a discrete minimal surface that has the same underlying topological structure as the initial surface M_0 and the surfaces M_i computed by the minimization algorithm (discrete maps preserve the structure).*

Remark 9. *For computing the minimum in step (2) a quadratic problem with non-linear side conditions arising from the restriction of the vertices to $\mathbb{S}^3$ has to be solved. We use a Conjugate Gradient method which was modified by the first author to allow minimization along spherical geodesics to solve this problem.*

4. Discrete cmc Surfaces via Conjugation

In this section we describe the conjugation process which takes a discrete minimal surface in $\mathbb{S}^3$ (a discrete harmonic map) and computes its corresponding discrete cmc surface in $\mathbb{R}^3$. We reserve the term *conjugation* for that process. In fact, we define conjugation already on the level of discrete harmonic maps, which – in contrast to discrete minimal surfaces – can be computed exactly with the methods of the previous section. This allows to conjugate any surface M_{i+1} (resp. discrete harmonic map F_i) computed with the minimization algorithm and avoids numerical difficulties in the conjugation of inaccurate minimal surfaces. Let us start with a definition of a discrete cmc surface.

Definition 12. *Let $M \in \mathfrak{T}(\mathbb{S}^3)$ be a discrete minimal surface and $F : M \to M$ the identity map, then the image of the conjugate map $F^* : M \to M^*$, $M^* \subset \mathbb{R}^3$ defined by definition 14 is called* a discrete constant mean curvature surface.

Remark 10. *This definition does not solely use a discrete version of the variational characterization of cmc surfaces, instead it characterizes discrete cmc surfaces by the discrete solution of their corresponding minimal surface problem in $\mathbb{S}^3$ together with a discrete version of lemma 1.*

With this approach our definition of a discrete cmc surface lies in-between a variational characterization of a discrete (minimal) surface in [14] which poses conditions on every vertex and an algorithmic definition of discrete (cmc) surfaces by Hoffman [11] who discretizes the Dorfmeister-Pedit-Wu method.

Of course one would like to estimate the distance of our cmc surfaces to solutions of a discrete variational problem but this is future work especially since our solutions are not triangulations, i.e. computing their area is not obvious.

When trying to simulate the differentiable conjugation process as described by lemma 1 several problems occur. Some of these problems can be solved using ideas from Pinkall/Polthier [14] for computing the dual of a Euclidean harmonic map while some others need special considerations of the Lie group structure of $\mathbb{S}^3$.

Let us start with the conjugation of a single atomic map

$$f : \triangle^N \to \triangle^M$$

between two triangles $\triangle^N \subset N$ and $\triangle^M \subset M$, $N, M \in \mathfrak{T}(\mathbb{S}^3)$. According to the definition of the C^1 conjugation in lemma 1 we will construct an equivalent of

$$f^{-1} {*df}$$

where f^{-1} is the left translation of the image and $*$ the Hodge star operator on the discrete level.

Instead of defining $*df$ on the whole triangle, we start with the definition of $*df$ at a vertex p of the triangle $\triangle^N$ (cf. figure 2). We use the projection operator

$$\pi_P : T_P\mathbb{R}^4 \to T_P\mathbb{S}^3$$

defined in (6) mapping vectors onto the tangent space at $P := f(p)$ to define the dual 1-form $*df_p$ at the point p by

$$*df_p(w) := P^{-1} \cdot \pi_P(df_p J_{\Delta^N} w)$$

where J_{Δ^N} is the rotation by 90° in the domain triangle Δ^N.

In words, we rotate the vector w in Δ^N by 90°, map it to $\triangle^M$, project it onto $T_P\mathbb{S}^3$ and left-translate it to the identity of $\mathbb{S}^3$, i.e. take the representative vector in the Lie-algebra. The definition of $*df_p$ obviously depends on the base point p and we cannot hope to extend $*df_p$ in a sensible way to the whole triangle. But the following lemma shows that $*df_p$ is in some sense independent of the base point, namely if applied to vectors w orthogonal to an edge through p.

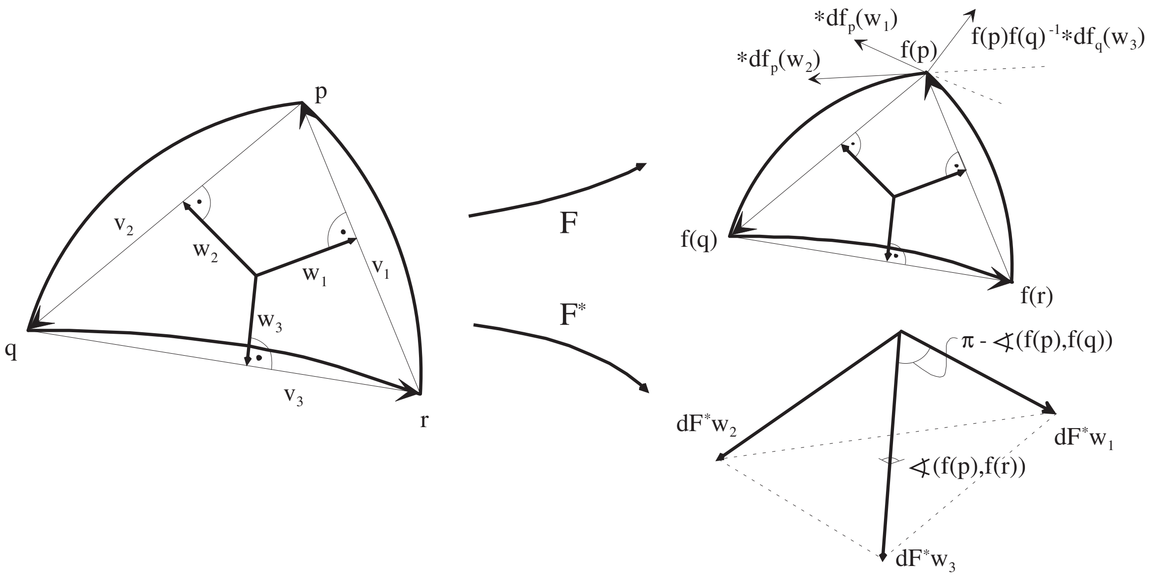

Figure 2: The dual 1-form $*dF$ is defined on the mid-perpendiculars in every triangle.

Lemma 13. *Let P and Q be two vertices of a triangle $\triangle^M$ joined in the domain by an edge v. Let $w \in T\triangle^N$ be a vector orthogonal to v, i.e. $J_{\Delta^N} w$ is parallel to v, then*

$$*df_q(w) = *df_p(w).$$

Proof. Since $\pi_Q(df_q J_{\Delta^N} w)$ points in the direction of the geodesic joining Q and P left translation by PQ^{-1} from $T_Q\mathbb{S}^3$ to $T_P\mathbb{S}^3$ will parallel translate $\pi_Q(df_q J_{\Delta^N} w)$ to $\pi_P(df_p J_{\Delta^N} w) \in T_P\mathbb{S}^3$. This proves the assertion.□

We could extend the definition of $*df_p$ to the whole triangle by linear extension but this would lead to ambiguities with $*df_q$ and $*df_r$ since only the application of two of these 1-forms to vectors orthogonal to their common edge gives the same result. Instead we use a case distinction in the following basic definition of the discrete conjugation:

Definition 14 [Discrete Conjugation]. *Let $F : N \to M$, $N, M \in \mathfrak{T}(\mathbb{S}^3)$ be a discrete harmonic map. Let $\triangle^N$ be a triangle in N and let v be an edge of Δ^N with endpoint p. Then the 1-form $*dF$ is defined on $T\triangle^N$ on vectors $w \in T\triangle^N$ orthogonal to the edge v by the action of the corresponding atomic dual 1-form. Let $f : \triangle^N \to \triangle^M$ be the corresponding atomic map then we define*

$$*dF(w) := *df_p(w) = P^{-1} \cdot \pi_P(df_p J_{\Delta^N} w). \tag{9}$$

In contrast to the Euclidean case of [14], where the dual 1-form of an atomic map could be defined as the smooth dual of the linear atomic map on the whole triangle, we must distinguish which base point we use for each triangle and therefore handle three cases. But we can proceed similar to the Euclidean case and show that our definition of $*dF$ gives a discrete 1-form which is continuous along certain paths and therefore can be integrated.

Lemma 15. *Let γ be the path around a vertex p on the discrete surface N consisting of the mid perpendiculars of the adjacent triangles (cf. figure 3). Then the 1-form $*dF$ is continuous along γ.*

Proof. It is sufficient to prove continuity across a single edge. Let $w_1, w_2 \subset \gamma$ be the two mid perpendiculars corresponding to the edge v of the adjacent triangles Δ_1^N and Δ_2^N. Then a direct trigonometric calculation yields

$$\begin{aligned} w_1 &= \cot\alpha \cdot J_{\Delta_1^N} v \\ w_2 &= \cot\beta \cdot J_{\Delta_2^N} v. \end{aligned}$$

If we apply $*dF$ (in every triangle we apply the dual 1-forms $*df_p$ or $*df_q$ of the atomic map) then we obtain

$$\begin{aligned} *dF(w_1) &= P^{-1} \cdot \pi_P(df_p J_{\Delta_1^N} w_1) = -P^{-1} \cot\alpha \cdot \pi_P(df_p v) \\ *dF(w_2) &= P^{-1} \cdot \pi_P(df_p J_{\Delta_2^N} w_2) = -P^{-1} \cot\beta \cdot \pi_P(df_p v). \end{aligned}$$

Therefore $*dF$ is continuous along paths γ orthogonal to edges.□

The following theorem proves the closedness of $*dF$, consequently the dual graph obtained by integration of $*dF$ is a well-defined discrete surface.

Theorem 16. *Let $F : N \to M$, $N, M \in \mathfrak{T}(\mathbb{S}^3)$, be a discrete harmonic map into $\mathbb{S}^3$ then the differential $*dF$ is closed along the path on N consisting of the mid perpendiculars of all triangles of N and integrates to a discrete surface in $\mathbb{R}^3$ whose edge graph is dual to the triangulation of N.*

If M is a discrete minimal surface in $\mathbb{S}^3$ and $F : M \to M$ the identity map then the discrete conjugate surface $\int *dF$ is a discrete CMC *surface in $\mathbb{R}^3$.*

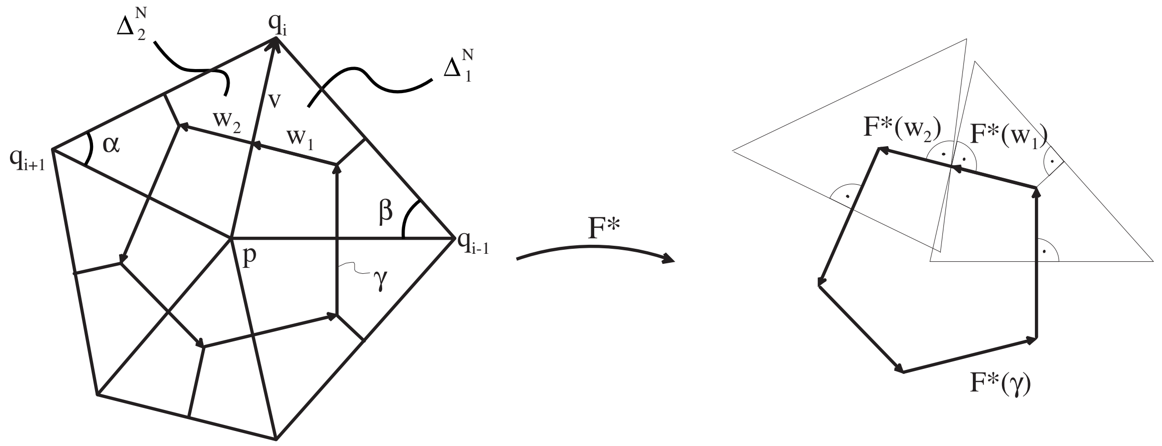

Figure 3: The dual map $F^* : N \to M^*$ is defined along certain paths γ orthogonal to edges. It associates to every vertex in N a dual cell in M^*.

Proof. Consider figure 3 and the piecewise linear closed path γ consisting of the mid perpendiculars adjacent to p. We integrate $*dF$ along γ:

$$\begin{aligned} \int_\gamma *dF &= P^{-1} \cdot \int \pi_P(df_p J\gamma') \\ &= -P^{-1} \cdot \sum_i (\cot\alpha_i + \cot\beta_i)\ \pi_P(Q_i - P) \\ &= 0. \end{aligned}$$

It turns out that the closedness condition for $*dF$ is identical to the harmonicity condition (7) for F, therefore for discrete harmonic maps definition 14 defines a continuous closed differential.□

Remark 11. *In practice we triangulate the obtained dual graph of the Euclidean* CMC *surface by defining an additional center vertex in each cell. Otherwise the continuation of the graph to the interior of the cells would be ambiguous and lead to problems during visualization.*

The following corollary shows the extreme discrete situations in which our algorithm is still applicable. Compare also the experiments with different discretization levels in section 6 – for the O,C-TO surface seven triangles suffice for a successful application of the algorithm.

Corollary 17. *Platonic solids with triangular faces and normalized so that the vertices lie on a great $\mathbb{S}^2$ are discrete minimal surfaces in $\mathbb{S}^3$. Applying our algorithm to these surfaces leads to discrete* CMC *surfaces in $\mathbb{R}^3$ which are the dual Platonic solids (i.e. discrete spheres).*

For example, the algorithm conjugates an octahedron (a discrete minimal surface in $\mathbb{S}^3$) to a cube (a discrete CMC *surface in $\mathbb{R}^3$).*

Remark 12. *A thorough study of convergence of our method is not completed and we hope to address it in a subsequent paper. Here we only remark that the discrete description of the conjugation defined in equation (9) converges to the smooth equation (2) when the discretization uniformly approaches zero.*

5. Conjugate Surface Construction and Symmetry

In this section we combine the methods we have developed in the previous sections to the conjugate surface construction which allows us to solve free boundary values problems for CMC surfaces in $\mathbb{R}^3$. We will only state the main facts without proofs since the arguments are of technical nature.

Symmetry properties of CMC surfaces are fundamental for the construction, therefore let us start with the following definition:

Definition 18. *Let M^* be a* CMC *surface with boundary segment δ^*. δ^* is called a* planar symmetry line *if it is a curve lying in a plane P and if M^* can be extended as a* CMC *surface by reflection in P.*

Let P be a (not necessarily convex) polyhedron whose boundary is a collection of planes $\partial P = \{p_i\}$. We want to construct a CMC disk-type patch M^* with free boundary $\Gamma^* = \bigcup \gamma_i^* \subset \bigcup p_j \subset \partial P$ where each arc γ_i^* is a planar symmetry line lying on some p_j. Suppose, there exists a solution M^* with boundary Γ^*, then by lemma 1 there exists a unique conjugate minimal surface $M \subset \mathbb{S}^3$ with polygonal boundary $\Gamma = \{\gamma_i\}$ where all γ_i are arcs of great circles in $\mathbb{S}^3$ and vice versa (compare remark 1). This correspondence can be used for a constructive approach, the conjugate surface construction. It's basic steps are:

(1) Determine the spherical contour Γ from the original boundary configuration ∂P of M^*.

(2) Compute the corresponding minimal surface $M \subset \mathbb{S}^3$ with boundary Γ.

(3) Conjugate M to a CMC surface $M^* \subset \mathbb{R}^3$.

For determining the contour Γ we need information about ∂P and the boundary curve of the wanted surface [12]. The dihedral angles of adjacent planes p_i, p_{i+1} determine the vertex angles of Γ (see remark 1), the total rotation of the normal along the boundary curve γ_i^* connecting two vertices is equal to the total rotation of the normal along the corresponding geodesic arc γ_i w.r.t. a left-parallel vector field. Therefore Γ is determined up to the lengths of the boundary arcs $|\gamma_i| = |\gamma_i^*|$. This leaves us with $n-3$ free parameters where n is the number of boundary segments $\{\gamma_i^*\}$ resp. planes in ∂P. Wrong choices of the $n-3$ parameters lead after conjugation to a CMC patch $\widetilde{M}^*$ which is bounded by a set of planes parallel to those of ∂P and not identical to them – the so-called period problem (cf. figure 5). To find the correct values for the parameters the construction can be executed repeatedly using a root finding algorithm.

Assume we have constructed the polygonal contour $\Gamma \subset \mathbb{S}^3$. It is a collection of arcs of spherical geodesics – each arc is part of a great circle. For the accuracy of the discrete conjugate surface construction it is essential to have an *exact* relationship of the boundary data of the numerically computed minimal surface in $\mathbb{S}^3$ with the corresponding data on the final conjugate discrete CMC surface in $\mathbb{R}^3$. The following theorem shows that already the intermediate discrete harmonic maps of the minimization algorithm lead to conjugate discrete surfaces in $\mathbb{R}^3$ which fulfil the boundary properties of the wanted CMC surface exactly – this is one of the most important results of our discrete definitions:

Theorem 19. *Let $\Gamma \subset \mathbb{S}^3$ be an n-sided polygonal boundary contour and $f : N \to M$, $N, M \in \mathfrak{T}(\mathbb{S}^3)$, a discrete harmonic map with the vertices of ∂N and ∂M lying on Γ. If Γ has vertex angles $\{\alpha_i\}_{i\in[1,n]}$ and normal rotation angles $\{\mu_i\}_{i\in[1,n]}$ (compared to a left-parallel vector field), then the conjugate discrete surface M^* has the following properties:*

(1) M^* has the same vertex angles α_i as M at the corresponding boundary vertices.

(2) The total rotation of the normal along the boundary arc γ_i^* of M^* is μ_i.

(3) The boundary arcs of M conjugate exactly to planar symmetry curves of M^* (this allows to extend M^* by reflection).

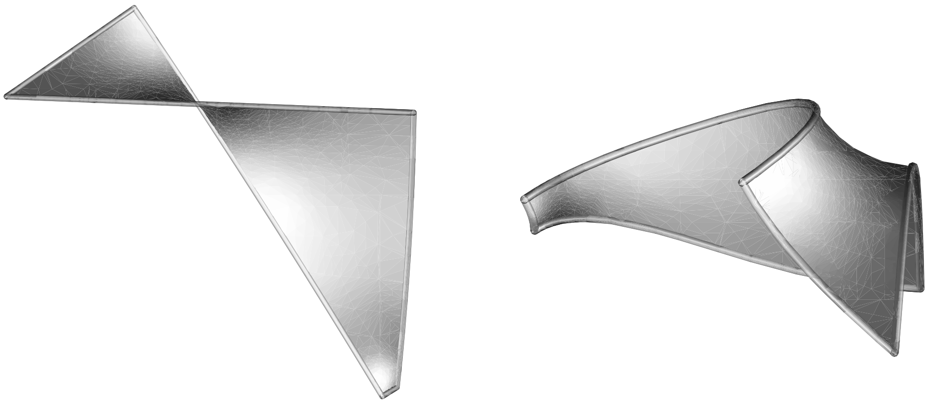

Figure 4: Two corresponding isometric fundamental patches for the conjugate surface construction. The picture on the left shows the polygonal contour in $\mathbb{S}^3$ bounding a minimal patch (stereographically projected to $\mathbb{R}^3$), the one on the right the conjugated CMC patch in $\mathbb{R}^3$. It can be extended by reflection at the planar boundaries to a complete CMC surface in $\mathbb{R}^3$, the O,C-TO surface shown in figure 6.

Remark 13. *Statements about the length of the conjugate boundary curve can only be made in the limit when the discretization approaches zero, then corresponding lengths are identical.*

Now we can combine our methods from sections 3 and 4 to a numerical algorithm, the *discrete conjugate surface construction*:

Problem: For a given (not necessarily convex) polyhedron P solve the free boundary value problem for a CMC surface in $\mathbb{R}^3$ with n boundary components $\Gamma^* = \{\gamma_i^*\} \subset \partial P$.

Discrete Conjugate Surface Construction:

(1) Using equations (1) and (2) replace the free boundary value problem by a Dirichlet boundary value problem for a minimal surface in $\mathbb{S}^3$ with boundary Γ. Extract from ∂P the information to determine the boundary Γ as a collection of spherical arcs $\{\gamma_i\}$ (up to $n-3$ parameters).

(2) Make a choice for the $n-3$ missing parameters.

(3) Apply the minimization algorithm from section 3 to obtain a sequence of discrete harmonic maps $\{F_i : M_i \to M_{i+1}\}$ such that $\{M_i\}$ converges to a discrete minimal surface $M \subset \mathbb{S}^3$. Since the algorithm stops after some finite number of iterations we obtain a discrete harmonic map $F_n : M_n \to M_{n+1}$ (M_{n+1} should be interpreted as an approximation of the discrete minimal surface M).

(4) Using theorem 16 compute the discrete conjugate harmonic map $F_n^* : M_n \to M_{n+1}^* \subset \mathbb{R}^3$ where M_{n+1}^* is a discrete approximation of the discrete CMC surface. By theorem 19 M_{n+1}^* fulfils boundary conditions $\partial\widetilde{P}$ which are identical to the required boundary conditions ∂P of the problem up to parallel displacement of the boundary planes.

(5) If $|\partial P - \partial\widetilde{P}| > \epsilon$ in some norm, start again with step (2) and a different guess for the $n-3$ parameters (in practice a root finding algorithm is used for the subsequent choices of these free parameters). Otherwise stop with a discrete CMC surface M^*.

Remark 14. *A major advantage of our algorithm is the fact, that we have defined the conjugation step (4) for the intermediate discrete harmonic maps and not only for the minimal surface M obtained in the limit in (3) since usually M cannot be computed exactly. Instead, the harmonic maps can be computed* exactly, *and therefore the conjugation algorithm for discrete harmonic maps does not accumulate errors.*

Remark 15. *When applying the algorithm to smooth problems there are two ways of enhancing the numerical accuracy: by choosing a finer discretization and by increasing the number of iterations for the minimization.*

Examples of discrete minimal and CMC surfaces computed with our algorithms are given in the next section and in [8] [7] [9].

6. Numerical Considerations and Visualization

For the development as well as applications of our algorithm visual control and interactive control of many parameters has been essential. In applications we usually consider one-parameter families of surfaces in a single experiment, this is for example always the case when a period problem has to be solved.

The algorithms are implemented in GRAPE [17], the mathematical visualization environment developed at the Sonderforschungsbereich 256 at the University of Bonn. Parameter-dependent surfaces are handled with the time concept of GRAPE: a family of surfaces is considered as a time-dependent process consisting of key-frames [16], intermediate surfaces are computed by linear interpolation. The GRAPE parameter "time" always refers to one specific parameter of the considered problem, for example to one of the free parameters (boundary curve lengths) of a geodesic polygon in $\mathbb{S}^3$.

A large number of tools, especially for creating and editing triangulations, was developed or extended for our algorithms using existing algorithms for other differential geometric surfaces, for example

- a surface builder for generating parameter-dependent surfaces in $\mathbb{S}^3$,
- visualization of surfaces in $\mathbb{S}^3$,
- curvature dependent adaptive refinement (this will result in varying discretization between key-frames while still allowing interpolation),
- reflection operations for the whole time-dependent surface family where the symmetry lines are allowed to change in time.

The minimization and conjugation algorithms and all tools for surfaces in $\mathbb{S}^3$ were implemented by the first author.

We cannot describe the techniques and numerical algorithms we use because of the restriction on the size of the paper and have to leave their discussion for a subsequent paper. Instead, in the following paragraphs we discuss the influence of the discretization and the number of iterations on the final CMC surface. Especially we consider the influence on the period problem since this is a critical quantitative question in practical applications.

As example surface we use the CMC companion of A. Schoen's Euclidean minimal surface O,C-TO which has one period to close. Its fundamental patch for the symmetry group is bounded by five symmetry arcs leading to a Plateau problem in $\mathbb{S}^3$ with five geodesic boundary arcs, see figures 4 and 5. We consider a sequence of three key-frames, the parameter called "time" controls the size of the handles growing at the centers of the six cubical faces, compare figures 5 and 6. To solve the period problem one has to find the time value at which the distance of the handle to the existing symmetry plane formed by the outer boundary arcs becomes zero (if the top of the handle is below the existing symmetry plane the period is negative, if it lies in the

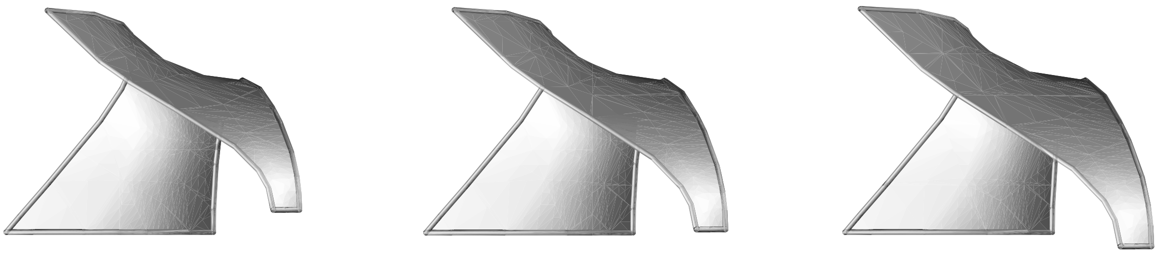

Figure 5: The three surfaces explain the period problem and graphically show the size of the period values in comparison with the size of the surface. The surfaces are the key-frames at times 0.0, 0.5 and 1.0 in the one-parameter family and correspond to the discretization with 291 triangles per fundamental patch in tables 1 and 2.

existing symmetry plane it is zero, otherwise it is positive). Since the fundamental patch has a second free parameter we get a family of CMC O,C-TO surfaces with varying mean curvature (after rescaling), see figure 8.

The discrete conjugation algorithm allows us to work with very coarse triangulations to handle the C^1 problem of conjugation (cf. corollary 17). During the minimization process there appears a degeneracy problem similar to the following example: when approximating a planar circular segment with a polygon, the polygon underestimates the length of the circular segment. When the polygon length is minimized the interior vertices of the polygon tend to move to the fixed end points, leading to a straight line in the limit. This kind of behaviour occurs during minimization in $\mathbb{S}^3$ on those surface parts with non-negative Gaussian curvature, i.e. spherical or cylindrical parts. If the surface is in principle stable, interactive local refinement

Iterations		1	10	50	100	250
Area	0.0	0.0670429	0.0670408	0.0670349	0.0670309	0.0670257
at	0.5	0.0746911	0.0746890	0.0746829	0.0746786	0.0746731
time	1.0	0.0828966	0.0828945	0.0828881	0.0828837	0.0828778
Period	0.0	-0.0203131	-0.0202376	-0.0202504	-0.0202911	-0.0203166
at	0.5	-0.0032060	-0.0031789	-0.0032184	-0.0032313	-0.0032676
time	1.0	0.0124860	0.0124902	0.0124475	0.0124341	0.0123958
zero at		0.6021510	0.6014435	0.6027202	0.6031350	0.6043069

Table 1: Dependency of the minimal surface area and the CMC surface period on the number of iterations for a fixed discretization of the fundamental patch with 291 triangles. The minimization algorithm converges rapidly during the first iterations; when the surface is close to its minimum the vertices try to move tangential to further decrease the energy and this motion is very slow. For the period problem and the final surface these last minimization steps seem to have qualitatively no influence, the intermediate time at which zero period occurs is very stable w.r.t. increasing number of iterations.

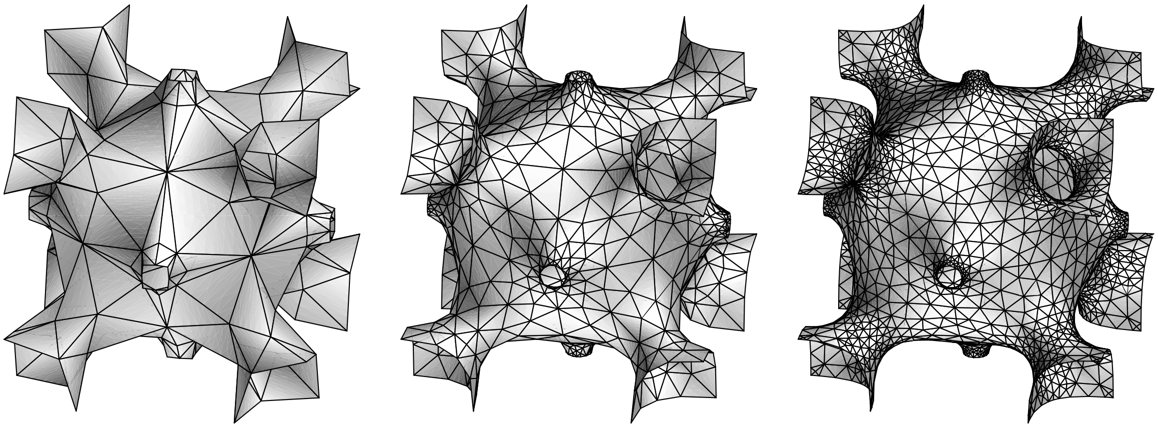

Figure 6: Discrete CMC versions of A. Schoen's O,C-TO surface with 7, 31 and 105 triangles per fundamental patch, the complete cell in a cube consists of 48 fundamental patches. For topological (not numerical) reasons less than 7 triangles seem to be impossible. The algorithm solves a C^1 problem for piecewise linear numerical data, and it is a great advantage of the discrete techniques that such coarse triangulations suffice.

depending on curvature terms can be used to eliminate these problems (at least for computing discrete harmonic maps). It should be mentioned that we use several methods to smooth the triangulations, this results in very good initial triangulations for the minimization.

It turns out that the numerical minimization algorithm converges rapidly during the first steps of the iteration and then slows down (after some steps the surface

Triangles		7	31	105	291	770
Area	0.0	0.0705462	0.0678702	0.0671622	0.0670408	0.0669850
at	0.5	0.0783776	0.0755613	0.0748169	0.0746890	0.0746309
time	1.0	0.0867911	0.0838075	0.0830244	0.0828945	0.0828342
Period	0.0	-0.0207651	-0.0228991	-0.0199642	-0.0202376	-0.0202183
at	0.5	-0.0022767	-0.0062105	-0.0028866	-0.0031789	-0.0031375
time	1.0	0.0097205	0.0092360	0.0127788	0.0124902	0.0125477
zero at		0.5948571	0.7010343	0.5921342	0.6014435	0.6000156

Table 2: Dependency of the minimal surface area and the size of the CMC surface period on different levels of discretizations after 10 iterations. The number of triangles is counted per fundamental patch, the part of the O,C-TO surface inside a cubical cell consists of 48 such fundamental patches. The values show that a coarse triangulation is sufficient for a qualitatively correct solution of the period problem. The intermediate time at which the zero period occurs is stable for triangulations which are not too coarse (more than ≈ 50 triangles in this case, compare the value for 31 triangles – for very coarse triangulations the value is not always as good as in this case).

vertices merely move tangential to minimize energy). Already the first iterates may be conjugated to give qualitatively and quantitatively good discrete CMC surfaces. In table 1 we list the dependency of the area of the spherical discrete surface and the size of the period of the CMC surface w.r.t. the number of iterations. The dependency of the area and period on the quality of the triangulation is analysed in table 2. Surely, the area of the spherical patch depends on the triangulation because we approximate with Euclidean triangles. But it turns out that the period depends very little on the discretization. The resulting surface in figure 6 is qualitatively correct even for the coarsest example.

REFERENCES

[1] A. Arnez, B. Oberknapp, K. Polthier, M. Steffens, and C. Teitzel. Visualization of time-dependent curves and surfaces. in preparation.

[2] A. Bobenko and U. Pinkall. Discrete isothermic surfaces. *J. reine angew. Math.*, 475:187–208, 1996.

[3] K. A. Brakke. The surface evolver. *Exp. Math.*, 1(2):141–165, 1992.

[4] K. A. Brakke and J. M. Sullivan. Using symmetry features of the surface evolver to study foams. In H.-C. Hege and K. Polthier, editors, *Visualization and Mathematics*, pages 95–117. Springer Verlag, Heidelberg, 1997.

[5] G. Dziuk. An algorithm for evolutionary surfaces. *Numer. Math.*, 58:603–611, 1991.

[6] K. Große-Brauckmann. New surfaces of constant mean curvature. *Math. Zeit.*, 214:527–565, 1993.

[7] K. Große-Brauckmann and K. Polthier. Numerical examples of compact surfaces of constant mean curvature. In B. Chow, R. Gulliver, S. Levy, and J. Sullivan, editors, *Elliptic and Parabolic Methods in Geometry*, pages 23–46, Wellesley (MA), 1996. AK Peters.

[8] K. Große-Brauckmann and K. Polthier. Constant mean curvature surfaces derived from delaunay's and wente's surface. In H.-C. Hege and K. Polthier, editors, *Visualization and Mathematics*, pages 119–134. Springer Verlag, Heidelberg, 1997.

[9] K. Große-Brauckmann and K. Polthier. Compact constant mean curvature surfaces with low genus. *Experimental Mathematics*, to appear 1997.

[10] M. Heil. Numerical tools for the study of finite gap solutions of integrable systems. Master's thesis, Technical University of Berlin, Berlin, 1995.

[11] T. Hoffmann. Discrete H-surfaces and discrete holomorphic maps. In A. Bobenko and R. Seiler, editors, *Discrete Integrable Geometry and Physics*. Oxford Press, in preperation.

[12] H. Karcher. The triply periodic minimal surfaces of A. Schoen and their constant mean curvature compagnions. *Man. Math.*, 64:291–357, 1989.

[13] H. B. Lawson. Complete minimal surfaces in S^3. *Ann. of Math.*, 92:335–374, 1992.

[14] U. Pinkall and K. Polthier. Computing discrete minimal surfaces and their conjugates. *Experim. Math.*, 2(1):15–36, 1993.

[15] K. Polthier. Geometric a priori estimates for hyperbolic minimal surfaces. *Bonner Mathematische Schriften*, 263, 1994.

[16] K. Polthier and M. Rumpf. A concept for time-dependent processes. In M. Göbel, H. Müller, and B. Urban, editors, *Visualization in Scientific Computing*, pages 137–153. Springer Verlag, 1995.

[17] Sonderforschungsbereich 256, University of Bonn. GRAPE *Manual*, Sept. 1995. Online information http://www-sfb256.iam.uni-bonn.de/grape/main.html.

Bernd Oberknapp
Sonderforschungsbereich 256
Institut für Angew. Mathematik
Universität Bonn
Wegeler Str. 6
53115 Bonn
Germany
Email: bo@iam.uni-bonn.de

Konrad Polthier
Technische Universität Berlin
FB 3 Mathematik, MA 8-3
Strasse des 17. Juni 136
10623 Berlin
Germany
Email: polthier@math.tu-berlin.de
WWW: http://www-sfb288.math.tu-berlin.de/~konrad/konrad.html

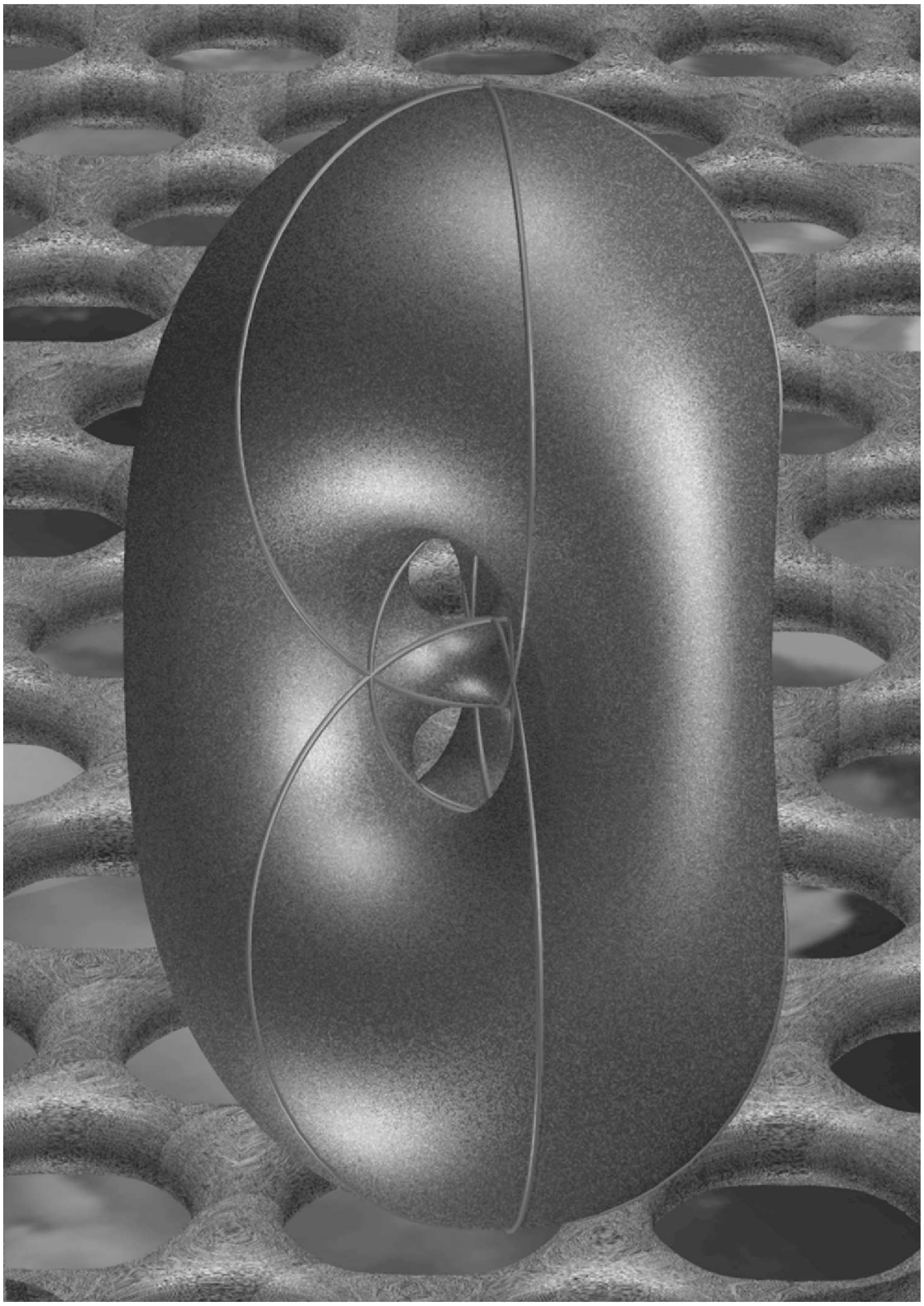

Figure 7: Lawson's compact minimal surface $\xi_{2,2}$ in $\mathbb{S}^3$ (stereographically projected to $\mathbb{R}^3$) computed with discrete techniques. The symmetry lines on the surface are great circles in $\mathbb{S}^3$, they divide the surface into 18 fundamental quadrilaterals with 60 degree angles. The associated constant mean curvature patch can be reflected to the doubly periodic surface on a hexagonal grid which is shown in the background.

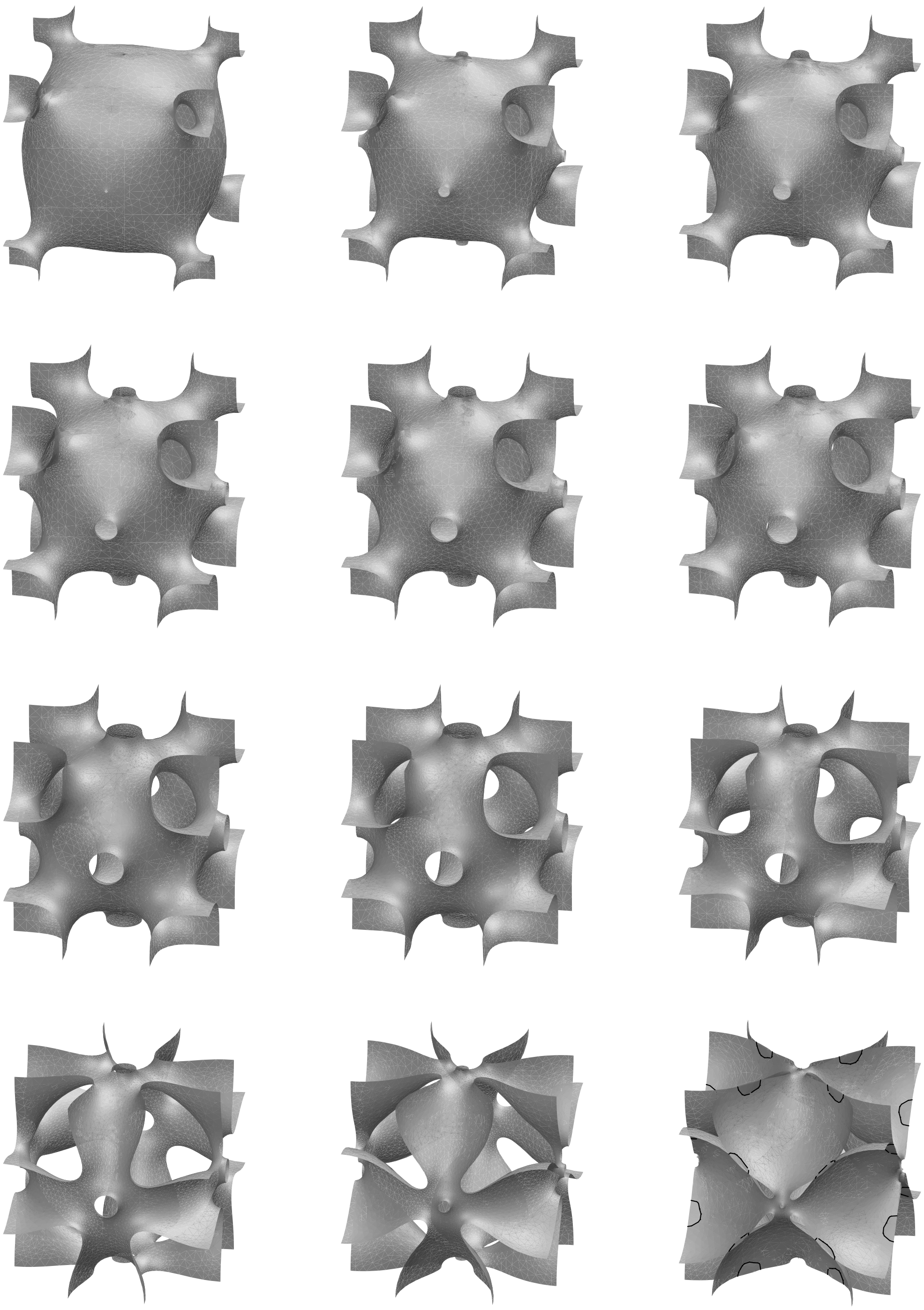

Figure 8: Discrete constant mean curvature companions of A. Schoen's O,C-TO minimal surface. The surface has two free parameters, one controls the distance (which is zero for this sequence) from the top of the handles at the centers of the cubical faces to the outer symmetry planes, the other one controls – after rescaling the surfaces – the mean curvature. At both ends of the sequence it is almost one, the O,C-TO minimal surface with zero mean curvature would be in the middle.